

On safety of lithium-ion cells

Ph. Biensan^{a,*}, B. Simon^a, J.P. Pérès^a, A. de Guibert^a, M. Broussely^b, J.M. Bodet^b,
F. Perton^b

^a SAFT, Direction de la Recherche, Route de Nozay, 91460 Marcoussis, France

^b SAFT, Advanced Battery Division, BP 1039, 86060 Poitiers, France

Abstract

Safety of lithium-ion cells is mainly related to thermal reactivity of the components. Active materials play a major role: carbon materials because they directly influence the kinetics of reactions at the negative electrode, positive materials because of their relation with their respective delithiation state. Adequately substituted nickel based materials appear as the most stable positive materials. Electrolyte is mainly concerned through its reactivity with lithium of Li_xC_6 and with O_2 generated by the positive materials decomposition. Moreover, non-active materials, in particular binders, also clearly influence thermal stability and consequently safety behaviour of lithium-ion cells. © 1999 Elsevier Science S.A. All rights reserved.

Keywords: Lithium-ion; Thermal stability; Safety; Materials

1. Introduction

Replacement of metallic lithium by a negative material able to intercalate reversibly lithium ions, so called lithium-ion, drove lithium secondary batteries to an undeniable commercial success. Negative carbon electrode (graphites, cokes, glassy carbons...), generally called Li_xC_6 , is currently the main developed technology. Together with the increase of cycle life and the fast charge acceptance compared to previous technology with metallic lithium, main improvement associated to the change of negative electrode is safety, even if some progresses have been described in a recent past with metallic lithium too [1].

Safety of lithium-ion in normal use is no longer questionable, which is not always true with metallic lithium because of dendritic deposit during charge. However, safety of lithium-ion must also be certified in case of abuse use. To overcome the eventual weaknesses and to improve safety, one must have a very good knowledge of all chemical reactions that may occur in case of unsafe behaviour.

2. Safety tests

Up to now, safety tests for lithium cells have been mainly developed for primary systems. Specific tests for lithium-ion cells with carbon negative electrode or more generally rechargeable lithium are currently under preparation in numerous important national and supranational organizations. The most recognized ones are edited by Underwriters Laboratories (UL-1642 or SU-2054), United Nations (UN) for transportation and International Electrotechnical Commission (IEC-project). Besides these three big organizations, others start to propose more specific standards, for example, those dedicated to military applications (United States Navy, French Army, German Army...). Other specific tests only exist for lithium primary cells, for space (British standard, AECMA...) or aeronautics (RTCA), for example. Japan Storage Battery Association (JBA) proposes a battery of specific tests for lithium batteries, widely followed today. UL is the only organizations to propose a test program for batteries which leads to a certification and authorization of the UR label (UL Recognized) in case of passing the tests. A cell or battery going through all the test may be considered as completely safe for the user. Main safety tests proposed by the different organizations are often adapted from UL ones, with some modifications of conditions and/or crite-

* Corresponding author

Table 1
Main safety tests proposed for lithium batteries

| Group | Main tests |
|---------------|--|
| Electrical | overcharge, overdischarge, external short-circuit, forced discharge... |
| Mechanical | drop, impact, nail, shock, crush, vibration, acceleration... |
| Thermal | flame, sandbath, hot plate, thermal shock... |
| Environmental | decompression, altitude, immersion, fungus resistance... |

ria for success, but others have been introduced specifically like the nail test by the JBA. Tests may be sorted in four groups as presented in Table 1.

All these tests are generally considered as representative of abnormal events that may occur in the frame of large scale production and commercialisation. The so-called nail test (pass from side to side a charged cell by a nail of specified dimensions) simulates an internal short-circuit or what a child would think about. Initially proposed by the JBA, this test starts being asked in the requirements of many consumers of lithium-ion cells. The overcharge represents a malfunction of the charger, which would not detect the end of charge of the battery. Environmental tests such as altitude or decompression simulate air transportation peculiar conditions, for example.

It is clear that all tests are not equivalent in terms of 'difficulty' to be passed with lithium-ion cells. Environmental ones may be considered as 'easy' tests, as well as overdischarge or external short-circuit for small cells. On the contrary, some tests are observed to be quite 'hard' to overcome: all those which induce a temperature increase in the charged state, whether heating is involving the whole cell (sand bath, hot plate or overcharge) or a very localized spot inside the cell due to an internal short-circuit (impact, nail, crush...). In the former case, thermal activation of chemical reactions introduces a self-heating of the cell which may bring it up to the point of no return (thermal runaway). In the latter, the temperature increase, locally created by the short-circuit, activates chemical reactions

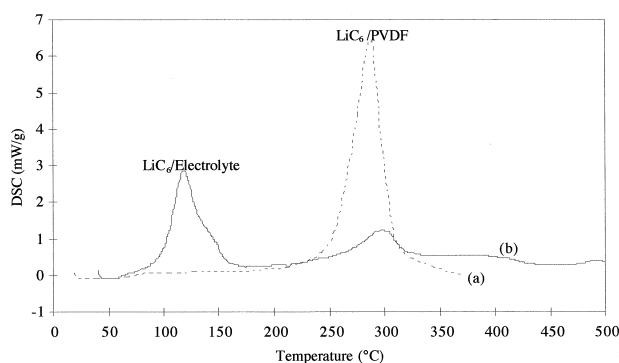


Fig. 1. DSC at 10°C/min on fully lithiated graphite electrode (a) without electrolyte, after rinsing—dotted line, (b) with electrolyte—full line.

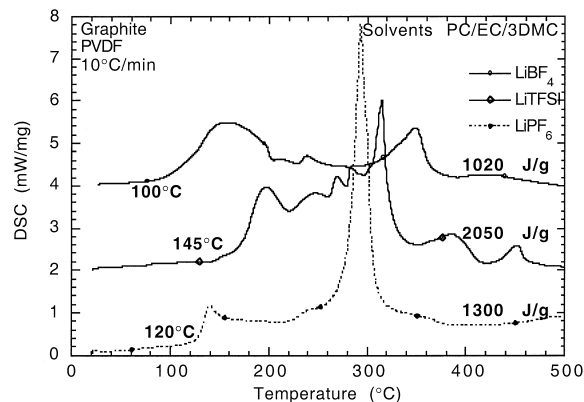


Fig. 2. DSC curves between room temperature and 500°C (10°C/min) of fully lithiated graphite negative electrodes for different salts at 1 mol/l concentration in the same solvent whose composition is PC/EC/DMC (1/1/3).

which may then propagate to the rest of the cell. In the following paper, we describe the study of the influence of some cell components on the thermally activated chemical reactions which play a first order role on the stability of $\text{Li}_x\text{C}_6/\text{Li}_y\text{MO}_2$ batteries. The possible chemical reactions, activated by the temperature increase whether local or general, will drive the cell to an undesired situation (thermal runaway, fire, explosion) only if the exothermic energy engaged is high, and if the kinetics of these reactions is elevated. If both conditions are not fulfilled, the reactions will be too weak or too slow to have violent consequences. Both aspects are considered here.

3. Study of temperature activated reactions

3.1. Introduction

All events which can lead to violent reactions in safety tests are observed in the charged state of lithium-ion batteries. Consequently, negative electrodes were studied

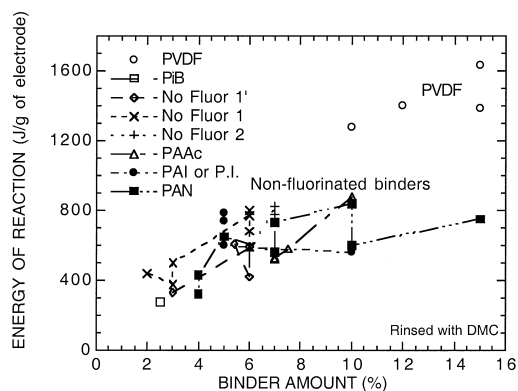


Fig. 3. DSC energy for the Li_xC_6 /binder reaction of fully lithiated graphite negative electrodes with different binders. Electrodes were rinsed several times with dry DMC prior to experiment.

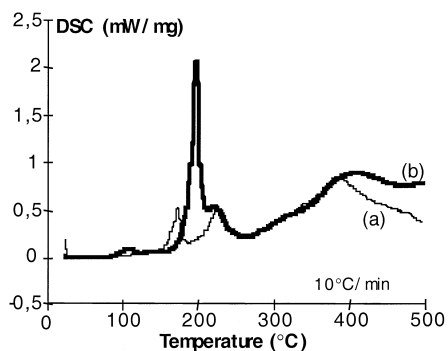


Fig. 4. DSC at 10°C/min on Li_xNiO_2 electrode charged at 4.1 V (a) without electrolyte, after rinsing with DMC, (b) with electrolyte.

in the fully lithiated state corresponding to Li_xC_6 ($x = 1$ for graphites) and positive electrodes in the delithiated state corresponding to the fully charged or overcharged state of the element.

The study of cells which failed different safety tests shows that the aluminium collector is melted but not the copper one, so that the reaction temperature, T_R , in the cell must be $T_{\text{Al}} = 659^\circ\text{C} \leq T_R \leq T_{\text{Cu}} = 1083^\circ\text{C}$, if one considers that T_R is similar for both electrodes: the minimum temperature in the coil is thus over 700°C , the temperature used in this paper for calculation of kinetics of reactions.

3.2. Experimental

Electrochemical cycling was made on a Mac Pile apparatus (BIO-LOGIC). Negative electrodes were lithiated at constant current (20 mA/g, 0.26 mA/cm^2) in laboratory coin cell with lithium counter electrode, and then saturated with lithium by short circuit between carbon and lithium counter electrodes. Positive electrodes were delithiated at constant current (6.9 mA/g , 0.17 mA/cm^2) in the same kind of cells, then charged at the desired constant voltage (4.1 V, 4.2 V...) during 20 h. The thermal stability studies of lithium-ion battery parts were undertaken by DSC (Differential Scanning Calorimetry, D50 from Shimadzu) in either aluminium or stainless steel crucibles, sealed at $P = 1 \text{ atm}$ under dry argon. For any thermal event, this experimental technique allows access to two parameters: (i) the endothermic or exothermic energy of reaction of the observed phenomenon and temperature of reaction and (ii) the kinetics of each reaction with Ozawa method [2]. This method was used to calculate the kinetic

parameters from DSC measurements made at different heating rates ($^\circ\text{C/min}$), i.e., the activation energy ΔE , the frequency factor A and the order of the reaction n from the general equation (Arrhenius):

$$dx/dt = A \cdot \exp(-\Delta E/RT)(1-x)^n \quad (1)$$

It is then possible for each reaction to calculate the energy flow as function of time at a given temperature (700°C) and then to compare the different reactions. Positive materials were also studied by differential thermal analysis coupled with mass spectroscopy (DTA + MS). DTA experiment was carried under argon at 10°C/min . Mass spectrometer was calibrated on $Z = 32$ for O_2 detection.

Experiments have been carried out on negative electrodes made from different carbons types. Electrodes were bound with PVDF unless otherwise specified. Several non-fluorinated binders were also studied with artificial graphite for the binder studies at the negative electrode. On the positive electrode side, LiNiO_2 (whether pure or substituted), LiCoO_2 and LiMn_2O_4 positive materials have been investigated. Electrodes were bound with PVDF. Unless otherwise specified, the electrolyte composition in all following studies is $\text{PC/EC/DMC}(1/1/3) + \text{LiPF}_6$ (1 M).

3.3. Results and discussion

3.3.1. Negative electrodes

Two different exothermic reactions appear on the DSC curve in Fig. 1, obtained for a lithiated artificial graphite negative electrode bound with PVDF. Onset temperatures of 120°C and 250°C roughly, in good agreement with the values measured by von Sacken et al. [3,4] or Zhang et al. [5], were measured. The study of the same electrode, rinsed with an inert volatile solvent (dry DMC) shows the disappearance of the first peak. If some electrolyte is added to the rinsed electrode, the peak reappears. An increase of crystallised products similar to those obtained from the reduction of electrolyte during the passivation (Li_2CO_3 , $\text{Li}_4\text{P}_2\text{O}_7$) of the electrode is observed by X-ray diffraction in presence of electrolyte. The first peak thus corresponds to the reaction between the lithium from LiC_6 and the electrolyte contained inside the porosity of the electrode. The maximum temperature of stability was also determined electrochemically for the passivation layer by cycling at increasing temperatures. The maximum tempera-

Table 2

DSC thermal behaviour of some positive materials from DSC compared to O_2 release temperature measured by DTA + MS (10°C/min , $Z = 32$)

| | LiNiO_2 | LiCoO_2 | LiMn_2O_4 | $\text{LiNi}_{(1-z)}\text{M}_z\text{O}_2$ |
|---|------------------|------------------|---------------------------|---|
| Capacity 1st charge/Reversible at 4.2 V or 4.3 V (Ah/kg) | 210/165 | 160/150 | 130/120 (4.3 V) | 205/160 |
| U_{max} for DSC slow kinetics (V) | < 4.1 | 4.3 | 4.7 | 4.7 |
| DSC main peak temperature with electrolyte ($^\circ\text{C}$) | 200 | 250 | 300 | 260/310 |
| Temperature of O_2 release ATG + MS ($^\circ\text{C}$) | 200 | 230 | 290 | 250/300 |

Voltages versus Li/Li^+ .

Table 3

Temperature of transformation to LiNi_2O_4 spinel was detected by X-ray diffraction, O_2 release by DTA + MS ($10^\circ\text{C}/\text{min}$, $Z = 32$)

| | $\text{Li}_{0.5}\text{MO}_2 \Rightarrow \text{LiNi}_2\text{O}_4$ | $\text{Li}_{0.3}\text{MO}_2 \Rightarrow \text{LiNi}_2\text{O}_4$ | O_2 release |
|---|--|--|---------------------------------|
| LiNiO_2 | 200°C | $< 170^\circ\text{C}$ | 200°C |
| $\text{LiNi}_{(1-z)}\text{M}_z\text{O}_2$ | 300°C | 250°C | $250\text{--}300^\circ\text{C}$ |

ture of stability is reached when coulombic efficiency does not reach 100% and this temperature corresponds to $100\text{--}120^\circ\text{C}$. The first peak observed by DSC is thus the consequence of the rupture of the passivation layer, which is no longer protective for the reaction between the electrolyte and the lithium intercalated into the carbon. This is confirmed by the influence of the electrolyte composition presented in Fig. 2: when the salt LiPF_6 is replaced by LiBF_4 or LiTFSI (Imide salt), the onset temperature as well as the energy of reaction is changed. LiBF_4 induces the lowest energy but also the lowest onset temperature ($< 100^\circ\text{C}$), while LiTFSI leads to the highest values for both onset temperature (145°C) and energy ($> 2000 \text{ J/g}$). LiPF_6 consequently appears as the best compromise.

The second peak was shown to be related to the reaction between the binder and the lithiated carbon: first, it disappears from the DSC curve for non-bound Li_xC_6 ; second, because the energy of reaction depends on the binder nature and amount. This latter point is illustrated in Fig. 3. First, the energy increases with the binder amount. Moreover, PVDF leads to two times more energy than the non-fluorinated binder it is compared to, for a similar amount (10–15% binder), in relation with LiF formation evidenced from X-ray diffraction studies.

The two reactions, with the electrolyte and with the binder, are in competition for the lithium consumption, as shown by the increase of the second peak energy when the first one is suppressed by rinsing with DMC in Fig. 1.

3.3.2. Positive electrodes

On the positive side, two different kinds of reactions have been observed too. Results are presented for $\text{Li}_{0.3}\text{NiO}_2$

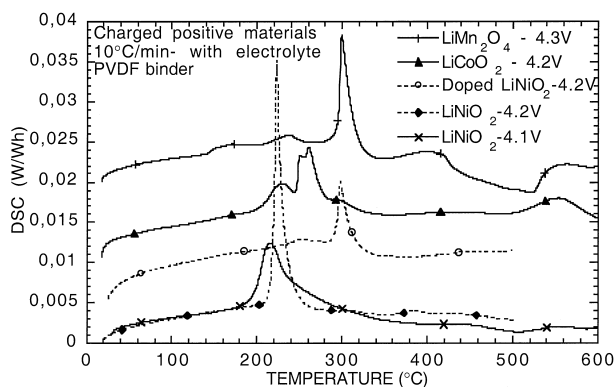


Fig. 5. DSC curves ($10^\circ\text{C}/\text{min}$) of $\text{Li}_y\text{Mn}_2\text{O}_4$, Li_yCoO_2 , Li_yNiO_2 , and $\text{Li}_y\text{Ni}_{(1-z)}\text{M}_z\text{O}_2$ in presence of electrolyte for specific end of charge voltages. Electrolyte is $\text{PC}/\text{EC}/\text{DMC}(1/1/3) + \text{LiPF}_6$ (1 M). Calculations are explained in the text.

in Fig. 4. First reaction corresponds to the positive material decomposition which appears clearly for the rinsed electrode. This phenomenon occurs in different steps: three exothermic peaks appear with peak temperatures of 180°C , 230°C and 380°C roughly; these temperatures are in good agreement with those measured by Dahn et al. [6]. They correspond to the progressive decomposition of Li_yNiO_2 . It was shown, by Differential Thermal Analysis associated with Mass Spectroscopy (DTA + MS) and X-ray diffraction, that positive material decomposition leads to oxygen release, to form $\text{Li}_{(1-x)}\text{Ni}_{(1+x)}\text{O}_2$ (Tables 2 and 3).

With electrolyte, a far more exothermic peak appears around 200°C with Li_yNiO_2 , superimposed to the material decomposition. The same study was carried out on Li_yCoO_2 , $\text{Li}_y\text{Mn}_2\text{O}_4$ and partially substituted $\text{Li}_y\text{Ni}_{(1-z)} \times \text{M}_z\text{O}_2$ materials. Results are summarized in Tables 2 and 3. This supplementary peak is attributed to the oxidation of

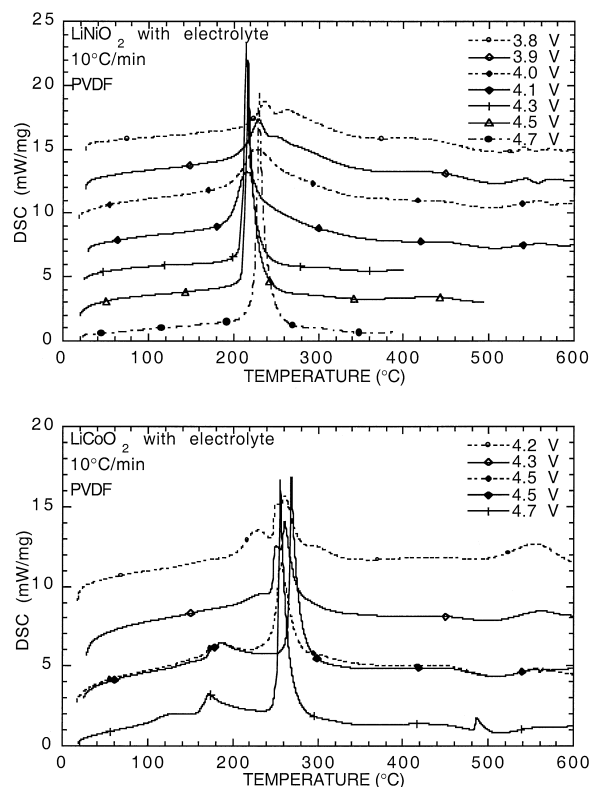


Fig. 6. DSC curves ($10^\circ\text{C}/\text{min}$) of Li_yNiO_2 (upper) and Li_yCoO_2 (lower) with electrolyte for various end of charge voltages. Electrolyte is $\text{PC}/\text{EC}/\text{DMC}(1/1/3) + \text{LiPF}_6$ (1 M).

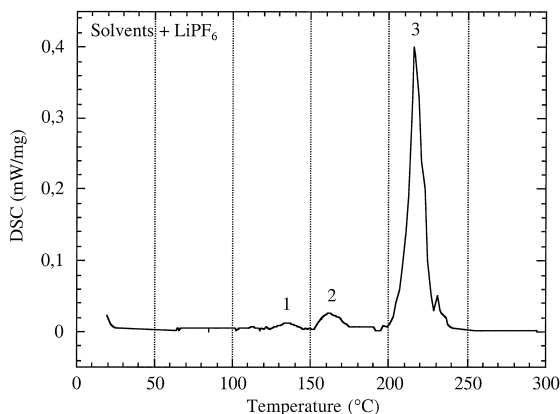


Fig. 7. DSC at 0.5°C/min of electrolyte PC/EC/DMC(1/1/3) + LiPF₆ (1 M).

the solvents by the oxygen because, whatever the positive material is, the peak occurs at similar temperature to the oxygen release observed by DTA + MS, as illustrated in Table 2. This is also true for substituted LiNi_(1-z)M_zO₂ material, for which the decomposition with oxygen release is shifted up to 250–300°C. Table 3 shows how partial substitution of Ni in LiNiO₂ allows to stabilize the material, increasing temperature of structural transition to spinel structure and temperature of oxygen release. Comparison between the positive materials is given in Fig. 5. The y scale is obtained by dividing the DSC specific power by the specific energy of each material, considering 180 Ah/kg–3.75 V, 150 Ah/kg–3.85 V and 120 Ah/kg–3.95 V for Ni, Co and Mn based materials, respectively and a first cycle efficiency (carbon) of 85%. The interest of the substituted nickel based materials appears clearly, with a high temperature of reaction (close to 300°C) and a smooth evolution of the peak, even with 4.2 V EOCV. The maximum W/Wh at the peak are even smaller than for LiMn₂O₄, related to higher capacity.

Influence of the delithiation state of positive materials was evaluated for each positive material. If no evolution is observed by DSC for Li_yMn₂O₄ between 4.3 V and 4.7 V

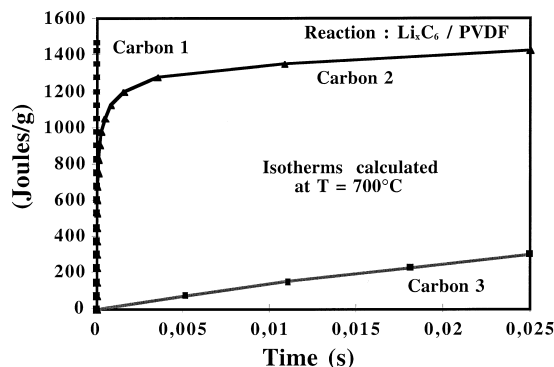


Fig. 8. Compared kinetics for reaction Li_xC₆/PVDF of three different types of carbons.

EOCV, Li_yNiO₂ and Li_yCoO₂ present a major change of the DSC curves shape, related to an important increase of the reaction rate with electrolyte (Fig. 6). This change occurs over 4.1 V vs. Li/Li⁺ for Li_yNiO₂ and 4.3 V vs. Li/Li⁺ for Li_yCoO₂. These voltages correspond roughly to the same delithiation state for both materials, which appears as the main reason for instability. Substituted LiNi_(1-z)M_zO₂ presents a higher temperature of reaction with the electrolyte, but also the kinetic of reaction remains smooth even at high end of charge voltages (4.7 V).

3.3.3. Electrolyte and separator

The electrolyte, PC/EC/DMC (1/1/3) + LiPF₆ (1 M), presents three different exothermic peaks between 130°C and 230°C (Fig. 7): these temperatures are lower than those measured by Hasegawa and Harakawa [7] for LiClO₄ (215°C) and LiCF₃SO₃ (260°C), implying a first order effect of the salt. The first two peaks are associated to a negligible energy. The main one, close to 215°C, corresponds to a total energy of 350 J/g of electrolyte: this value remains however small comparatively to the one measured for both electrodes.

For separators, the main thermal event measured by DSC corresponds to the fusion of the polymer. The phenomenon is endothermic and thus it will not induce any

Table 4
Energy of main reactions for lithium-ion accumulator measured by DSC

| | Temperature range (°C) | Reaction | Energy (J/g) | Comment |
|-----|------------------------|---|--------------|--------------------------------|
| 1 | 110–150 | Li _x C ₆ + electrolyte | 350 | Rupture of passivation layer |
| 2 | 130–180 | Fusion separator P.E. | –190 | Endothermic |
| 2' | 160–190 | Fusion separator P.P. | –90 | Endothermic |
| 3 | 180–500 | Decomposition of Li _{0.3} NiO ₂ + electrolyte | 600 | Oxygen emission peak T ≈ 200°C |
| 3' | 220–500 | Decomposition of Li _{0.45} CoO ₂ + electrolyte | 450 | Oxygen emission peak T ≈ 230°C |
| 3'' | 150–300 | Decomposition of Li _{0.1} Mn ₂ O ₄ + electrolyte | 450 | Oxygen emission T ≈ 300°C |
| 4 | 130–220 | Solvents + LiPF ₆ | 250 | Low energy |
| 5 | 240–350 | Li _x C ₆ /PVDF binder (rinsed) | 1500 | Violent-propagation |
| 6 | 660 | Fusion of aluminium | –395 | Endothermic |

Electrolyte was PC/EC/DMC(1/1/3) + LiPF₆ (1 M).

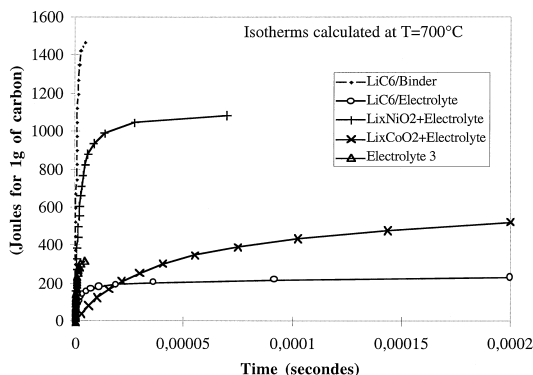


Fig. 9. Kinetics of main exothermic reactions of an accumulator $\text{Li}_x\text{C}_6/\text{Li}_y\text{MO}_2$: u, $\text{Li}_x\text{C}_6/\text{binder}$; +, $\text{Li}_y\text{NiO}_2/\text{Electrolyte}$; \times $\text{Li}_y\text{CoO}_2/\text{Electrolyte}$; o, $\text{Li}_x\text{C}_6/\text{Electrolyte}$; s, Electrolyte 3 (equilibrated cell, calculation for 1 g of carbon).

degradation of the thermal stability of the cell. However, the energies measured are very small (-90 J/g for PP and -190 J/g for PE).

Contribution of the different components of a carbon/electrolyte/ LiMO_2 accumulator are summarized in Table 4. Different exothermic reactions lead to high energies. The two main reactions identified are associated, one to the positive electrode (with electrolyte), and the second to the negative one ($\text{Li}_x\text{C}_6/\text{PVDF}$). On the other hand, endothermic fusion of separators or of aluminium collector have small contributions. The negative electrode, with reactions 1 and 5, generates more energy (1850 J/g) than the positive one.

3.3.4. Kinetics aspects

Kinetic measurements by Ozawa method allow a direct comparison of the role of each material. As an example, negative electrode carbons with different levels of crystallinity have been studied. Fig. 8 shows the calculated advancement of reaction at 700°C for $\text{Li}_x\text{C}_6/\text{binder}$ reaction of three carbons fully lithiated: y scale is obtained by the product of the energy measured by DSC by the advancement of reaction, which variation versus time is calculated from Eq. (1). Kinetics are really different for the three carbons, even if the total energy involved is roughly

the same. These results imply that the carbon nature rules the kinetic of the chemical reactions at the negative electrode. X-ray diffraction studies show that the reaction occurs at the surface of the carbon with no change of crystalline structure (parameters, coherence lengths...): reactions are thus limited by the maximum diffusion rate of lithium out of the carbon. Results obtained by Way and von Sacken [8], via ARC, confirm the influence of the carbon type on the self-heating rate of the negative electrode. On the other hand, the heat flow limitation observed by Menachem et al. [9] (by creating a chemically-bonded solid electrolyte interface (CB-SEI) on the graphite) means that this CB-SEI tends to improve safety by lowering the kinetic of lithium diffusion out of the carbon. Fig. 8 shows the very high rate of heat generation, since reaction is almost complete after ~ 5 ms for carbon2 mixture at 700°C .

Fig. 9 compares the heat generation rates of reactions 1, 3–3b, 4 and 5 from Table 4: all energies are related to 1 g of carbon for an equilibrated lithium-ion cell (same capacity per surface unit for positive and negative electrodes). Calculation are made for a carbon1/PVDF negative electrode, with either $\text{LiNiO}_2/\text{PVDF}$ or $\text{LiCoO}_2/\text{PVDF}$ and PC/EC/DMC(1/1/3) + LiPF_6 (1 M) electrolyte. Kinetic parameters extracted by the Ozawa method are used to calculate the heat generation rate at 700°C (isotherm). Results clearly demonstrate that, moreover the important energy generated by the negative electrode, the kinetics of both reactions at this electrode are higher than those at the positive one, even with LiNiO_2 material (4.1 V vs. Li/Li^+). Even if the differences in specific capacities imply a higher weight of positive material, negative electrode remains the most exothermic. Secondly, the electrolyte self-reaction contribution is small. The most violent reaction appears to be between the lithium stored into the carbon and the negative electrode binder.

3.3.5. Validation in complete cells

Nail tests on 4/5A cells (450–500 mAh) have been used as validation test of the above results. Cells were made with the materials described in Table 5. Electrolyte

Table 5
Nail test results for different electrochemical definitions in 4/5A cells

| Negative material | Negative binder | Positive material LiMO_2 | Positive binder | Safe voltage (V) |
|-------------------|-----------------|---|-----------------|------------------|
| Carbon 1 | PVDF | LiCoO_2 | PVDF | 4.0 |
| Carbon 3 | PVDF | LiCoO_2 | PVDF | 4.5 |
| Carbon 1 | PVDF | LiNiO_2 | PVDF | 3.65 |
| Carbon 3 | PVDF | LiNiO_2 | PVDF | 3.9 |
| Carbon 1 | No Fluor 1 | LiCoO_2 | PVDF | 4.3 |
| Carbon 1 | No Fluor 1 | LiNiO_2 | PVDF | 3.95 |
| Carbon 1 | No Fluor 2 | LiNiO_2 | PVDF | 3.95 |
| Carbon 1 | No Fluor 2 | $\text{LiNiO}_2 + \text{LiCoO}_2$ | PVDF | 4.0 |
| Carbon 1 | No Fluor 2 | Optimized $\text{LiNi}_{(1-z)}\text{M}_z\text{O}_2$ | PVDF | 4.2 |

No Fluor 1 and 2 correspond to two different formulations with non-fluorinated binders.

was PC/EC/DMC(1/1/3) + LiPF₆ (1 M) and Celgard 2300 was used as separator. Different cells were nailed after being charged at increasing voltages until thermal events were observed. The voltage range comprise between 3.5 V and 4.5 V was investigated. The maximum safe voltage (for which there was no leakage, no vent, no fume, no fire) for each cell definition appears in the last column of Table 5. All parameters identified from the DSC studies, such as the kinetics of reaction at the negative electrode (different carbons), the binder nature (fluorinated or not), the positive material (LiNiO₂, LiCoO₂, LiNi_(1-z)M_zO₂), clearly impact on the maximum safe voltage of the cell. The change of negative electrode carbon material from carbon1 to carbon3 increases the maximum safety voltage to at least 300 mV. A same increase is observed when PVDF is replaced by a non-fluorinated binder in the negative electrode. Substituted nickel based material improves the safety voltage up to 4.2–4.3 V for the nail test, when associated with a negative electrode bound with non-fluorinated binder.

4. Conclusions

This work confirms DSC as a very useful tool for safety improvement of lithium-ion cells. Associated with the Ozawa method, it allowed us to measure and compare the kinetics of temperature activated reactions involved. The sorting in terms of energy and kinetics shows that both electrodes contribute to the thermal instability of lithium-ion cells. For the negative, the energy is controlled by the nature and amount of binder, the composition of electrolyte and the lithiation state of the carbon. On the other hand, the kinetic is controlled by the lithium diffusion out

of the carbon. On the positive side, the energy is controlled by the type of material (Ni, Co, Mn) and its delithiation state through the amount of oxygen produced during its decomposition, whereas the kinetics are mainly influenced by the state of delithiation (EOCV) and the substitution nature for LiNi_(1-y)M_yO₂. For both electrodes, electrolyte plays an important role on the high potential reactivity. The results obtained demonstrate also that non-active materials like binders have to be optimized too, if one wants to improve the thermal stability of this electrochemistry.

Acknowledgements

The authors wish to thank the DGA (Direction Générale de l'Armement) for financial support.

References

- [1] P. Dan, E. Mengeritski, Y. Geronov, D. Aurbach, I. Weisman, J. Power Sources 54 (1995) 143–145.
- [2] T. Ozawa, J. Thermal Anal. 2 (1970) 301.
- [3] U. von Sacken, E. Nowdwell, A. Sundher, J.R. Dahn, Solid State Ionics 69 (1994) 284–290.
- [4] U. von Sacken, E. Nowdwell, A. Sundher, J.R. Dahn, J. Power Sources 54 (1995) 240–245.
- [5] Z. Zhang, D. Fouchard, J.R. Rea, Electrochem. Soc. INC Fall meeting abstracts, San Antonio 96-2, pp. 168–169.
- [6] J.R. Dahn, E.W. Fuller, M. Obrovac, U. von Sacken, Solid State Ionics 69 (1994) 265–270.
- [7] K. Hasegawa, Y. Arakawa, J. Power Sources 43–44 (1993) 523–529.
- [8] B.M. Way, U. von Sacken, Electrochem. Soc. INC Fall meeting abstracts, San Antonio 96-2, pp. 1020–1021.
- [9] C. Menachem, D. Golodnitsky, E. Peled, Electrochem. Soc. meeting abstracts, Paris 97-2, pp. 157–158.